Evaluation of windowing techniques for intramuscular EMG-based diagnostic, rehabilitative and assistive devices

Ashraf, Hassan; Waris, Asim; Gilani, Syed Omer; Kashif, Amer Sohail; Jamil, Mohsin; Jochumsen, Mads Rovsing; Niazi, Imran Khan

Published in:
Journal of Neural Engineering

DOI (link to publication from Publisher):
10.1088/1741-2552/abcc7f

Publication date:
2021

Document Version
Accepted author manuscript, peer reviewed version

Evaluation of windowing techniques for intramuscular EMG-based diagnostic, rehabilitative and assistive devices

To cite this article before publication: Hassan Ashraf *et al* 2020 *J. Neural Eng.* in press https://doi.org/10.1088/1741-2552/abcc7f

IOP Publishing Journal Title
Journal **XX** (XXXX) XXXXXX https://doi.org/XXXX/XXXX

Evaluation of Windowing Techniques for Intramuscular EMG-based Diagnostic, Rehabilitative and Assistive Devices

Hassan Ashraf [1] · Asim Waris [1] · Syed Omer Gillani [1] · Amer Sohail Kashif [1] · Mohsin Jamil [2] · Mads Jochumsen [3], and Imran Khan Niazi [3,4,5]

[1] Department of Biomedical Engineering and Sciences, School of Mechanical and Manufacturing Engineering (SMME), National University of Science and Technology (NUST), 44000, Islamabad, Pakistan.
[2] Department of Electrical and Computer Engineering, Faculty of Engineering and Applied Science, Memorial University of Newfoundland, NL, A1B 3X5, St John's, Canada.
[3] Department of Health Science and Technology, Aalborg University, 9220 Aalborg, Denmark.
[4] Center of Chiropractic Research, New Zealand College of Chiropractic, 1149, Auckland, New Zealand.
[5] Faculty of Health and Environmental Sciences, Health and Rehabilitation Research Institute, AUT University, Auckland 0627, New Zealand.

E-mail: asim.waris@smme.nust.edu.pk
Received xxxxxx
Accepted for publication xxxxxx
Published xxxxxx

Abstract

Objective. Intramuscular electromyography (iEMG) signals, invasively recorded, directly from the muscles are used to diagnose various neuromuscular disorders/diseases, and to control rehabilitative and assistive robotic devices. iEMG signals are being potentially used in neurology, kinesiology, rehabilitation, and ergonomics, to detect/diagnose various diseases/ disorders. Electromyography (EMG) based classification and analysis systems are being designed and tested for classification of various neuromuscular disorders and to control rehabilitative and assistive robotic devices. Many studies have explored parameters, such as pre-processing, feature extraction and selection of classifier that can affect the performance and efficacy of iEMG-based classification systems. Pre-processing stage includes removal of any unwanted noise from original signal and windowing of the signal. *Approach.* This study investigated and presented optimum windowing configurations for robust control and better performance results of iEMG-based analysis system based on stationarity rate and and classification accuracy. Both, disjoint and overlap, windowing techniques with varying window and overlap sizes have been investigated using a machine learning (ML) based classification algorithm called linear discriminant analysis (LDA). *Main results.* The optimum window size ranges are from 200ms to 300ms for disjoint and 225ms to 300ms for overlap windowing technique, respectively. The inferred results show that for overlap windowing technique the optimum range of overlap size is from 10% to 30% of the length of a window size. Mean classification accuracy (MCA) and mean stationarity rate (MSR) was found to be lower in disjoint windowing technique as compared to overlap windowing at all investigated overlap sizes. Statistical analysis (two-way analysis of variance test) showed that MSR and MCA of overlap windowing technique was significantly different at overlap sizes of 10% to 30% (p-values < 0.05). *Significance.* The presented results can be used to achieve best possible classification results and stationarity rate for any iEMG based real-time diagnosis, detection, and control system which can enhance the performance of the system significantly.

Keywords: Windowing, Classification, Machine Learning, Electromyography

1. Introduction

Electromyography (EMG) is an electrical activity associated with muscles contraction generated due to underlying motor neurons. EMG can be recorded by Intramuscular (invasive) and/or Surface (non-invasive) recording techniques. Surface EMG (sEMG) is recorded from surface of the skin whereas intramuscular EMG (iEMG) is recorded directly from the muscle that generates electrical activity. The EMG produces an electric field in its surroundings and enables recording relatively away from the source [1]. Biological tissue that separates recording electrode from the source is referred as volume conductor and behaves as a low-pass filter [2]. iEMG allows to record EMG from relatively near vicinity of the source and thus the effect of volume conductor is minimum as compared to sEMG. There are various applications of EMG-based techniques; these have potentially been used to detect nervous system disorders in Neurology, to detect psychological and physical stress/disorders along with detection of musculoskeletal disorders in Ergonomics, to provide an insight for exercise physiology in Kinesiology, and to control rehabilitative and assistive robotic devices in Rehabilitation [3]. Myoelectric control schemes are being designed by mainly relying on sEMG signals due to their non-invasive recording techniques. But the systems designed using iEMG signals provide sensory control and feedback to body more efficiently [4].

Whether the aim is to analyze EMG signals for diagnostic applications or to develop EMG-based control system for rehabilitative or assistive devices, windowing is of crucial importance. Windowing is a process that divides recorded EMG signals into smaller parts to analyze fine characteristics of the signal. The windowing process is used in decomposition of EMG signals, and also to design myoelectric control schemes for rehabilitative and assistive devices [5-7]. Classification and identification of action potentials by virtue of individual motor units through analyzing interference pattern is called EMG signal decomposition. Two steps are required for decomposition of composite EMG signal in classic approaches i.e. 1) detecting action potentials by using windowing and ii) recognition of detected action potentials as a member of specific class [8-10].

Currently, iEMG is being used with additional advancements like implantable electrodes [11, 12]. Therefore, this has now become much easier to identify the parameters that can affect performance of an iEMG based classification system. Multiple studies have been conducted to assess parameters affecting performance of EMG-based control system [13-21]. But a limited research has been conducted to explore abilities and efficacy of iEMG signals. Herberts et al. (1968) for the first time in history recorded iEMG signals using telemetry system from 4 subjects for control purpose and measured contraction levels by applying various loads [22]. Stein et al. (1980) implanted 4 electrodes to control upper limb prostheses and reported to have a greater control [23].Various studies have been conducted to explore the efficacy of iEMG recordings for prosthetic and rehabilitative assistive robotic controls, however, no study has explored the optimum windowing configurations for iEMG-based control systems [23-25]. Goen (2013) used iEMG signals for classification of neuromuscular disorders (Normal, myopathic and neuropathic) by using data recorded from 34 subjects (22 pathogenic and 12 normal) with sampling frequency of 2 kHz [26]. Various EMG features were investigated by deploying disjoint window with window size of 200 sampling points. The results showed that support vector machine (SVM) outperformed other investigated classifiers and achieved an accuracy of 91.2%. Another study conducted by Subasi et al. (2018) used iEMG signals, recorded at sampling frequency of 20 kHz, from 27 subjects for automatic detection of various neuromuscular disorders [27]. The recorded iEMG data was segmented using a disjoint window with window length of 1024 samples. The authors reported that, the SVM achieved highest classification accuracy of 98.96% among other investigated classifiers. Yaman and Subasi (2019) recorded iEMG signals with sampling frequency of 20 kHz and decomposed recorded signals for the classification of neuromuscular disorders [28]. The authors utilized disjoint window with window length of 2048 samples to extract various features. Based on the extracted features, the authors reported that the artificial neural network (ANN) achieved highest accuracy of 98.33% among other investigated classifiers. All these studies used fixed window size without investigating the impact of window size on stationarity rate and classification accuracy.

Bioelectric or physiological signals, generated from body due to any physiological activity are windowed according to their shape so that each window can represent actual activity of that area or muscle. For example, electrocardiography (ECG) is a bioelectric signal generated due to contraction and relaxation of heart, representing activities of cardiac muscle. It is segmented according the shape or pattern of the signal to represent activities of the heart. Unlike ECG, EMG signals cannot be segmented according to their shape due to their stochastic nature. Rather, these signals are segmented by length of time. A single window should be long enough in time to contain enough information that represent the pattern of original signal. Oskoei et al. (2008) reported that, for EMG signals, a window length of 200ms provides significant information for accurate representation of original signal [29]. Smaller windows have more variance and less bias whereas larger windows have more bias and less variance. Besides variance and bias, there are other factors that should

be taken in account during windowing process of EMG signals; such as its real-time performance of operation, computational load, and accuracy of the designed system. All these parameters get affected greatly by length of the window size in classification of EMG signals. Larger window sizes provide better performance in classifying EMG signals but real-time operation of any such system restricts to keep window size below 300ms for natural and robust performance of the device [30]. Furthermore, windowing of EMG signals can be done by using disjoint or overlap windowing techniques. In disjoint windowing technique, the window is only characterized by window size whereas in overlap windowing a window is characterized by window size and step/overlap size. Figure 1 describes the two types of windowing techniques. The step or overlap size should be greater than operation time of the device and less than the window size. Overlap windowing thus allows to use larger window sizes, as compared to disjoint window, without any delay in real-time operation of the device.

Staionarity of the signals plays an important role in signal processing. As stated earlier, EMG signals are nonstationary and are segmented by length of time rather than shape. The nonstationarity causes complexities and affect the results catastrophically, specifically, when dealing with frequency analaysis [31]. The prerequisite for frequency analysis i.e. Fourier Transform, Wavelet Transoform and various Signal Decomposition techniques is that the signal under consideration should be stationary. A shorter segment of EMG signal can be locally stationary. For sEMG signals various studies have shown that shorter segments possess stationarity [32-34]. Beck et al. (2006) conducted a study to test the stationarity of the sEMG signals using RUNS test, Reverse Arrangement (RA) test, and Modified Reverse Arrangment (MRA) test [35]. Similarly, Messaoudi et al. (2017) tested the stationarity of the synthetic sEMG signals with respect to various disjoint window sizes and conluded that the window size of 225ms exhibits the maximum stationarity rate [36].

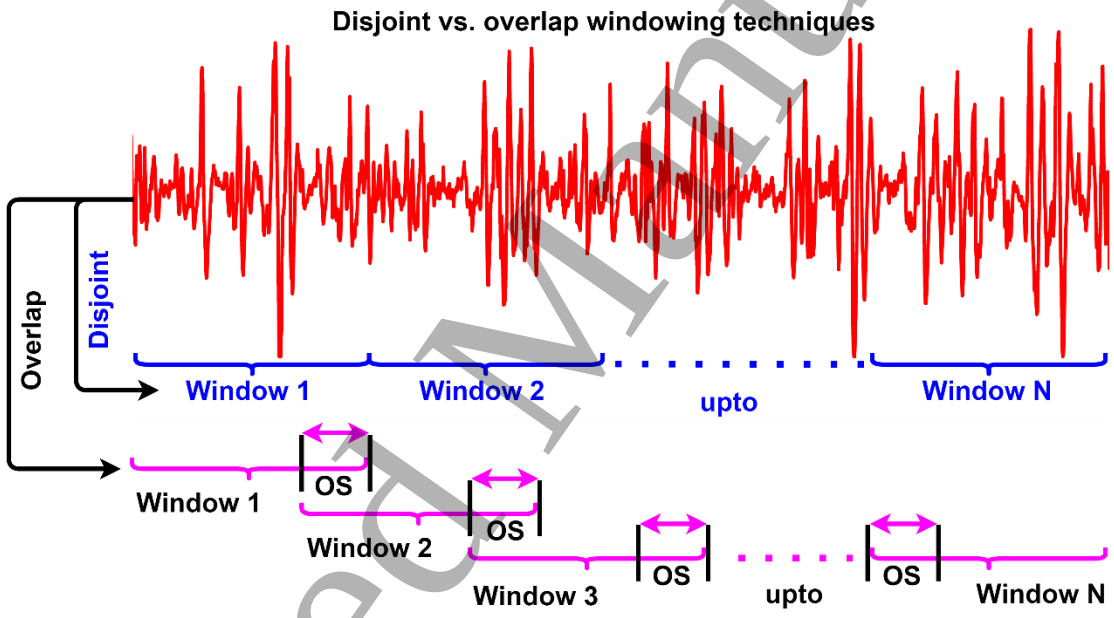

Figure 1. Shows the difference between disjoint and overlap windowing techniques. The preprocessed EMG signal, is segmented into distinct segments, as shown in blue color fonts, in disjoint windowing technique. Whereas, in overlap windowing technique, each window is characterized by window size and overlap size (OS). The overlap is the portion of the segment overlapping between two consecutive windows.

Any myoelectric control based rehabilitative and assistive robotic device should decode the EMG signal in less than 300ms for natural and robust control of the device [37]. Similarly, for diagnostic and detection purposes the window size plays an important role in decoding and preserving the exact shape of motor unit action potential (MUAP). In clinical practice, the clinicians use a window size of 200ms to 300ms to examine the shape of MUAP for detection and diagnosis of various neuromuscular diseases [38,39]. No study has ever explicitly evaluated the optimum windowing configuration for an iEMG-based classification and control system for enhanced performance. The role of stationarity rate, for an iEMG-based analysis system, in determining optimum window type, window and overlap size is also yet to be explored. For sEMG-based control systems, it is evident that windowing type and window size have a great effect on the performance of the designed system [37]. As we have previously shown that the overlap windowing technique outperforms disjoint windowing for a sEMG-based myoelectric control and optimum windowing configurations

were presented for both windowing techniques [32]. The mentioned literature has revealed much information and promising results but most of the studies revolve around sEMG signals and for an iEMG-based diagnosis, detection, and control system there is no consensus on selection of window size. Various studies used various windowing techniques (Disjoint or Overlap), window and overlap sizes either with respect to time length or number of samples based on the sampling frequency of the data.

The aim of this study is to investigate optimum windowing configurations for iEMG-based control system with respect to stationarity rate and performance of the system. Both windowing techniques with varying window sizes have been investigated using linear discriminat analysis (LDA) classifier. The effect of length of overlap or increment size, for overlap windowing technique, on stationarity and performance of an iEMG-based classification and control system has also been investigated. Three independently recorded datasets of iEMG recordings of hand motions have been used for generalization. The significance of the results has been evaluated using analysis of variance statistical analysis. The criteria followed to choose an optimum window size is that the selected window size should provide maximum stationarity rate and classification accuracy while adhering the real-time constraints of window size (less than 300 ms) [41]. The selected window size should also have a balanced variance-bias tradeoff and the length of chosen overlap size should be greater than the processing time of the device and less than the window size while resulting maximum stationarity rate and classification accuracy.

The rest of the study has been organized as: the detailed information about iEMG recordings, experimental paradigm, and methodology of the study is described in section 2. Section 3 describes results of all conducted experiments along with their statistical comparison. Section 4 discuss and interpret the achieved results and section 5 provides overall conclusion of the presented study.

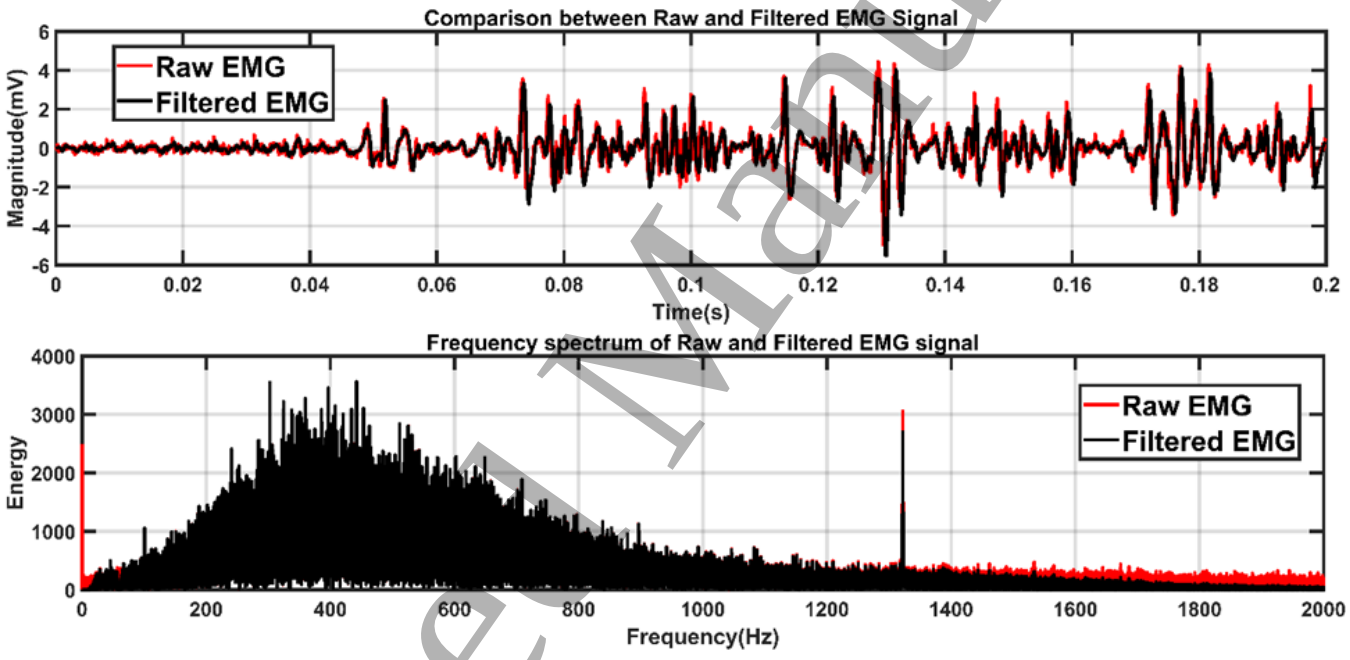

Figure 2. Shows the comparison between recorded and filtered EMG signal. Signals in time domain (Top), and and signals in frequency domain (Bottom). In both graphs, the signal plotted with red and black colors are raw and filtered EMG signals, respectively.

2. Methodology

25 (healthy and amputee) subjects participated in this study. Three independently recorded datasets were used. In all three datasets, iEMG signals from upper limbs were recorded. Dataset-1 is comprised of 10 healthy subjects and had been used in [9]. Dataset-2 with recordings from 8 healthy subjects was also pre-recorded and had been used in [19]. Whereas, dataset-3 was comprised of 5 amputees which had different level of transradial amputation. The details about dataset-3 can be aquired at [9].

2.1 Dataset-1

iEMG recordings for dataste-1 were recorded using 6 bipolar stainless-steel electrodes coated with Teflon (A-M Systems, Carlsborg WA diameter 50 µm). The wire electrodes were inserted into flexor carpi radialis, palmaris longus, flexor carpi ulnaris, extensor carpi radialis longus, flexor carpi radialis brevis and flexor digitorum superficialis muscles.

The insertion of wire electrodes was made possible using a sterilized 25-guage hypodermic needle. The needles were inserted into designated muscles to a depth of approximately 10-15mm so that wire electrodes can stay inside the muscles for a specific time. An ultrasound scanner was also used to identify required muscles and for correct placement of electrodes. To avoid the risk of infections, all the precautionary measures were used. Skin, wire electrodes and needles were sterilized. The tips of inserted wire electrodes were then connected to amplifier (AnEMG12, OT Bioellectronica, and Torino, Italy) to amplify signals. The signals were filtered (20-1500 Hz) with an analog bandpass filter and sampled at 8 kHz sampling frequency using 16-bit NI-DAQ card.

The subjects performed ten active hand motions and rest motion (REST) which is a no-motion state. Active hand motions including Hand Open (HO), hand Close (HC), Wrist Flexion (WF), Wrist Extension (WE), Pronation (PRO), Supination (SUP), Side Grip (SG), Fine Grip (FG), Agree (AGR) and Pointer (POI) were performed by each subject. To record data a graphical user interface (GUI), BioPatRec, a publicly available data acquisition and pattern recognition, software was used [37]. To make it easy for subjects each motion was graphically visualized on computer screen before recording. Each subject performed experiment in such a way that at start of the experiment the subject kept hand at rest for 5 seconds and then performed the displayed motion for 5 seconds by contracting muscles. After each contraction of 5 seconds the subject had to perform REST for 5 seconds and so on.

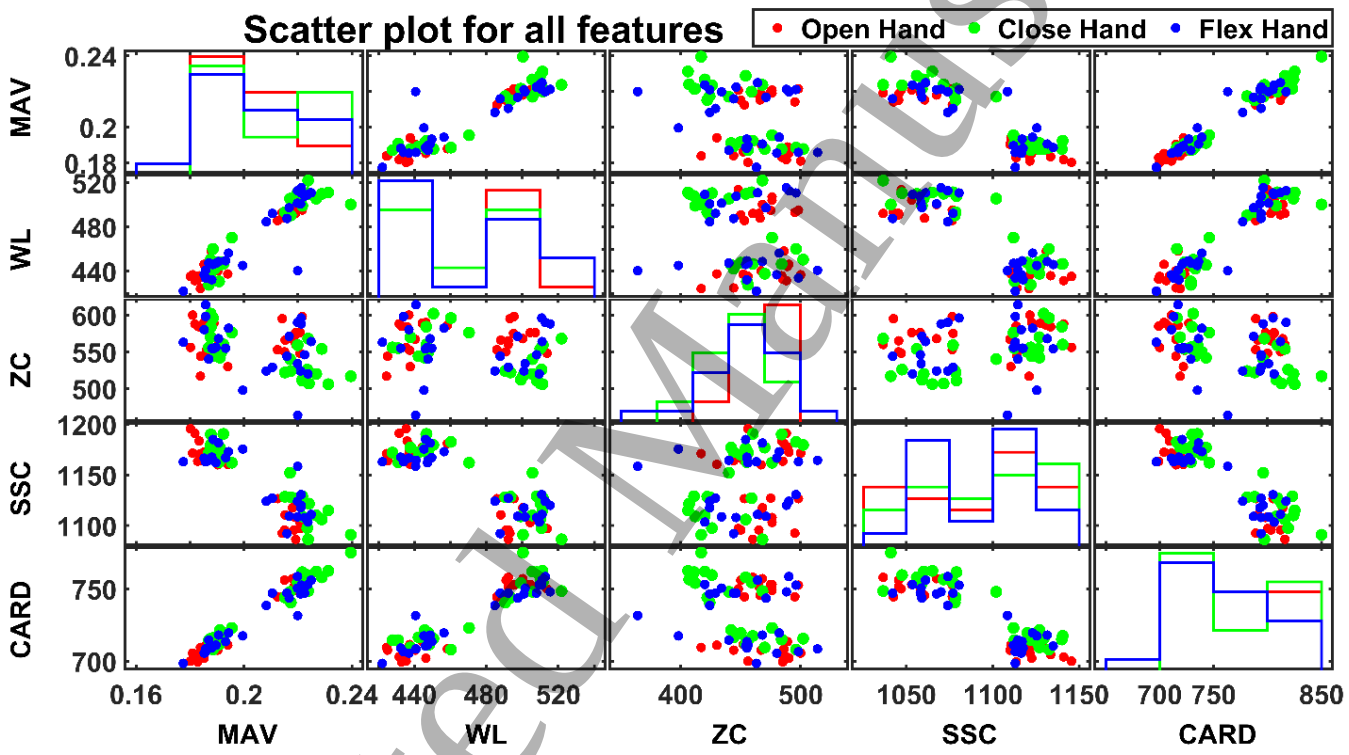

Figure 3. In the scatter plot for all the extracted features, x-axis of the leftmost column corresponds to MAV feature. Y-axis of the bottom row corresponds to CARD feature. The scatter plot in the bottom left of the matrix compares MAV values (along the x-axis) to CARD values (along the y-axis). The color of each point depends on the hand motions (red, green, and blue represents HO, HC, and HF, respectively.). The diagonal plots are histograms showing the feature values for each hand motion.

2.2 Dataset-2

The dataset-2 was also pre-recorded and sampled at sampling frequency of 10 kHz, it has been used previously in [19]. The participants of this dataset performed following 4 active hand motions: HO, HC, WF and WE along with REST.

2.3 Dataset-3

The dataset-3 was also pre-recorded and sampled at sampling frequency of 8 kHz, it has been used previously in [9]. The data collection protocol was same as dataset-1, the wire electrodes were inserted around the circumference of the forearm, equidistantly.

2.4 Signal processing

Signals from all datasets were digitally filtered using a third-order Butterworth bandpass filter using cut off frequencies of 20 Hz and 1500 Hz. Also, a notch filter of 60 Hz was used to cancel out the effects of power line interference. The signal recorded during contraction time was used to extract features, excluding the signal recorded during transient time. Figure 2 depicts the comparison between both raw and filtered EMG signals, from dataset-1, in time and frequency domain. It can be observed that applied digital filters significantly remove embedded noise from the original signal.

2.4 Windowing

To investigate which windowing technique, window size and step/overlap size provides best classification results for EMG signals, the recorded datasets were segmented by using both windowing techniques. For both techniques 19 different window sizes were used, such that the length of window size varied from 25ms to 500ms with an increment of 25ms. Similarly, for overlap windowing 9 different step/overlap sizes were used from 10% of original window length to 90% with an increment of 10% in length of overlap size.

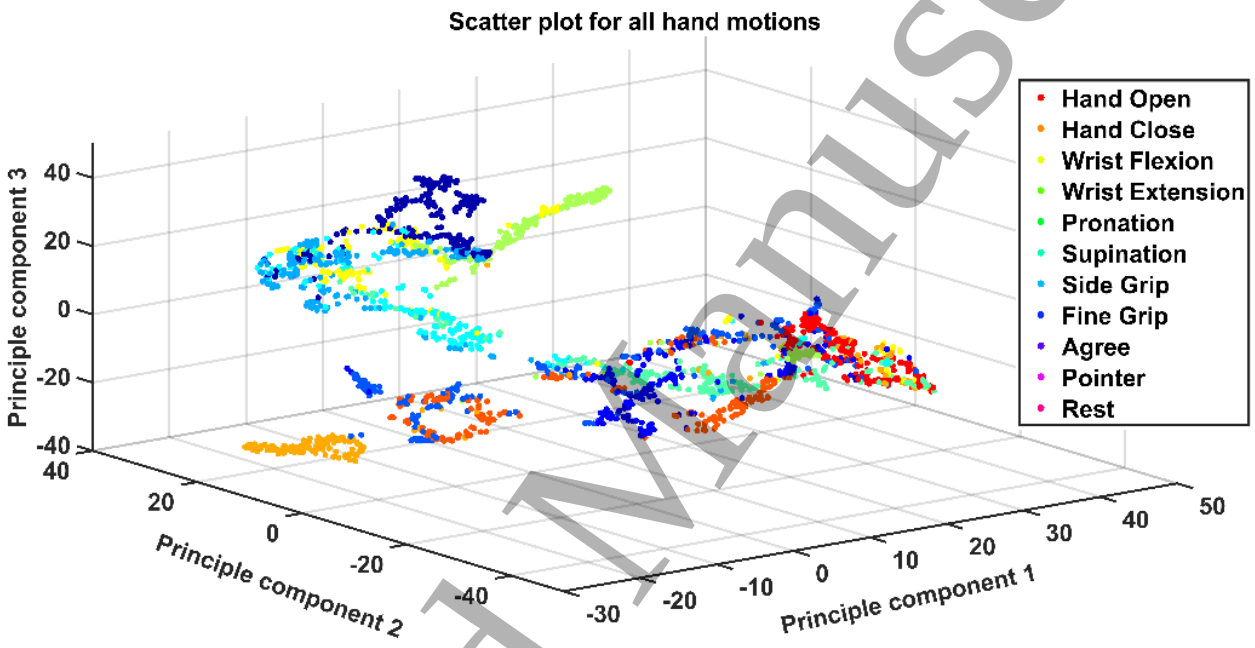

Figure 4. 3-Dimenional scatter plot for hand motions. PCA reduces the dimensionality of the data to prevent Over-fitting through elimination of redundant features. To decrease dimensionality to 3 dimensions, PCA and TSNE algorithms have been used. X-axis of the leftmost column corresponds to MAV feature. Y-axis of the bottom row of corresponds to CARD feature. Bottom left compares MAV values (along the x-axis) to CARD values (along the y-axis). The color of each point depends on the hand motions (red, green, and blue represents HO, HC, and HF, respectively.). The diagonal plots are histograms showing the feature values for each hand motion.

2.5 Stationarity of iEMG

A stationary process which has a spsecific state of statistical equilibrium such that its marginal distribution does not depends on time and its bivariate distribution depends on time difference or lag. These stated assumptions implies that the variance and mean of the signal are constant and the autocorrelation is dependent on time difference. Any stochastic process which satisfies the mentioned properties of a stationary process is called as wide sense stationary (WSS) process or simply a stationary process. To test which windowing technique, window size and overlap size provides the maximum stationarity for iEMG signals, all the windowed signals were first used for stationarity test. The stationarity of the segments were evalauted using two statistical stationarity tests i.e. RUNS test and Reverese Arrangment (RA) test. A segment was considered stationary only if a segment is proven stationary from both tests. The stationarity of each window or overlap size is reported in terms of stationarity rate. The stationarity rate is defined as

the number of total statioanry signals divieded by total number of signals.

2.6 Feature extraction

After windowing, next step was to extract useful information from each window that can distinguish window of one class from another. For this purpose, various statistical properties of EMG signals were calculated to represent original signal. These statistical properties (features) should possess the capability of class separability and can be computed from frequency or time domain. In time domain, features are evaluated with respect to amplitude of signal. However, in in frequency domain the same are calculated from power spectral density (PSD). Selected feature set, chosen for EMG classification, should have an ability of maximum class separability, minimum computational complexity, and high robust power. Apropos, 5 TD features have been investigated in this study i.e. mean absolute value (MAV), waveform length (WL), slope sign change (SSC), cardinality (CARD) and zero crossing (ZC). The scatter plot of all extracted features for 3 hand motions (HO, HC, and WF) for one subject from dataset-1 is depicted in figure 3.

Another factor that affects the performance of ML based system is overfitting of designed system. System designed with larger feature set is prone to over-fit. An overfitted ML model fits too closely (exactly) to a specific dataset, but fails to predict unseen features on the new dataset. To prevent overfitting, Principle Component Analysis (PCA) has been used. PCA removes redundant features and maps from high dimensionality to low dimensionality preserving the variance. Figure 4 depicts a 3-dimensional scatter plot for all hand motions with reduced dimensionality. For visualization, the dimensionality of the feature set has been reduced by utilizing PCA and T-distributed Stochastic Neighbor Embedding (TSNE) algorithm.

2.7 Classification

Finalized feature set was then fed to LDA to classify iEMG signals of various classes. To evaluate performance of the classifier classification accuracy (CA) has been measured. For each dataset, windowing technique, and window size, a classifier was trained, validated, and tested for each subject. The data of each subject was divided in such a way that 70% of data was used to train the model, 20% for validation and the remaining 10% was used to test the trained model. LDA was used from publicly available MATLAB toolbox "BioPatRec" for EMG signals [41]. The CA of testing results were measured and recorded for each subject. To assess effects of window size and windowing technique on performance of classification of iEMG signals, analysis of variance (ANOVA) test was used. Probability values below than 5% were considered significant for evaluation of the statistical tests. Furthermore, for multiple comparisons among the variables Tuckey's honest post-hoc test was also used.

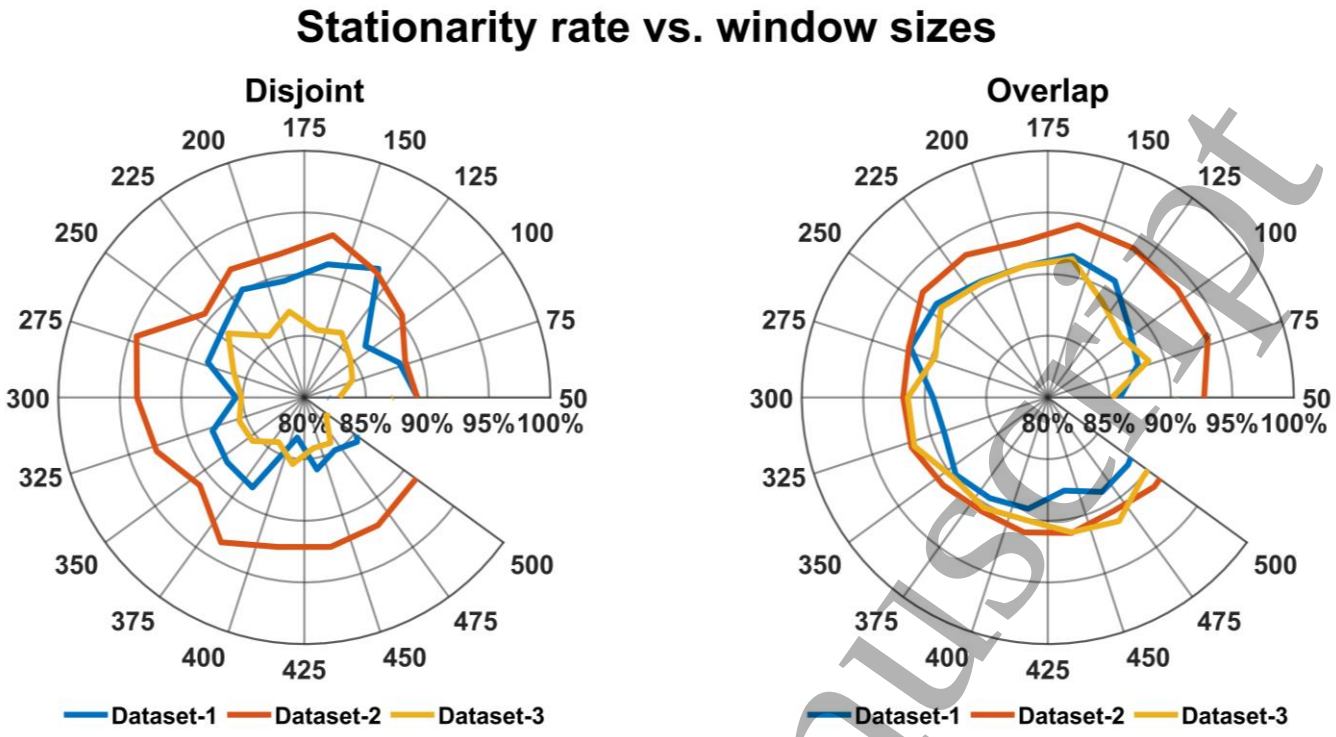

Figure 5. SR vs. window sizes for disjoint and overlap windowing. Relationship between SR and length of disjoint segments for all datasets (Left). Relationship between SR and length of window size for overlap windowing (Right).

3. Results

The LDA classifier was trained and tested for both datasets, windowing techniques, against each window size. Classification accuracy (CA) and Stationarity Rate (SR) of each individual subject was recorded based on all motions/classes. By averaging CA of all subjects, in both datasets, mean classification accuracy (MCA) was calculated. Similarly, mean stationarity rate (MSR) was calcuated. The results are presented as MCA±STD and MSR±STD.

3.1 Optimum window sizes

To investigate optimum window sizes for both disjoint and overlap windowing, 19 different window sizes with varying lengths (50ms to 500ms) have been chosen for both windowing techniques. It should be noted that, as overlap windowing is characterized by a window size along with a step/overlap size, MCA and MSR of all 9 overlap size is averaged to get mean of MCA (MMCA) and mean of MSR (MMSR) for any given window size for fair comparison. Figure 5 depicts the relationship between MSR and increasing length of window size for both windowing techniques on all datasets. It can be observed that MSR increases with an increment in window size from 50ms to 500ms. Similarly, figure 6 depicts the relationship between MCA and window sizes.

For disjoint windowing technique, the highest MSR of 90.96%, 94.51% and 87.07% resulted against window size of 150ms, 250ms and 175ms for dataset-1, dataset-2 and dataset-3, respectively. Two-way ANOVA showed that for all datasets, using disjoint window technique, no statistical difference among MSR of all window sizes exist (P-values > 0.05). With respect to CA, for datasets 1, the lowest and highest MCA were recorded at window size of length of 50ms and 475ms with MCA of 83.62%±4.6 and 92.5%±6.16, respectively. The MCA significantly increased from 83.62%±4.6 to 91.03±3.1, as the window size is changed from 50ms to 200ms. Afterwards, increment in window size from 200ms to 500ms does not increase MCA significantly (only an increment of 1.47%). For dataset-2, the highest and lowest MCA of 96.35%±3.3 and 99.17%±1.52 were recorded at window size of 50ms and 275ms, respectively. MCA significantly increased by increasing window size from 50ms to 275ms and afterwards no significant change occurs in the MCA of dataset 2. For dataset-3, the lowest and highest MCA were observed at window size of 50ms and 400ms with MCA of 73.36% and 91.34%, respectively. The MCA significantly increased from 73.36%±13.2 to 87.02%±8.9 by changing window size from 50ms to 250ms, however, no significant increment in MCA has been observed by increasing window size afterwards.

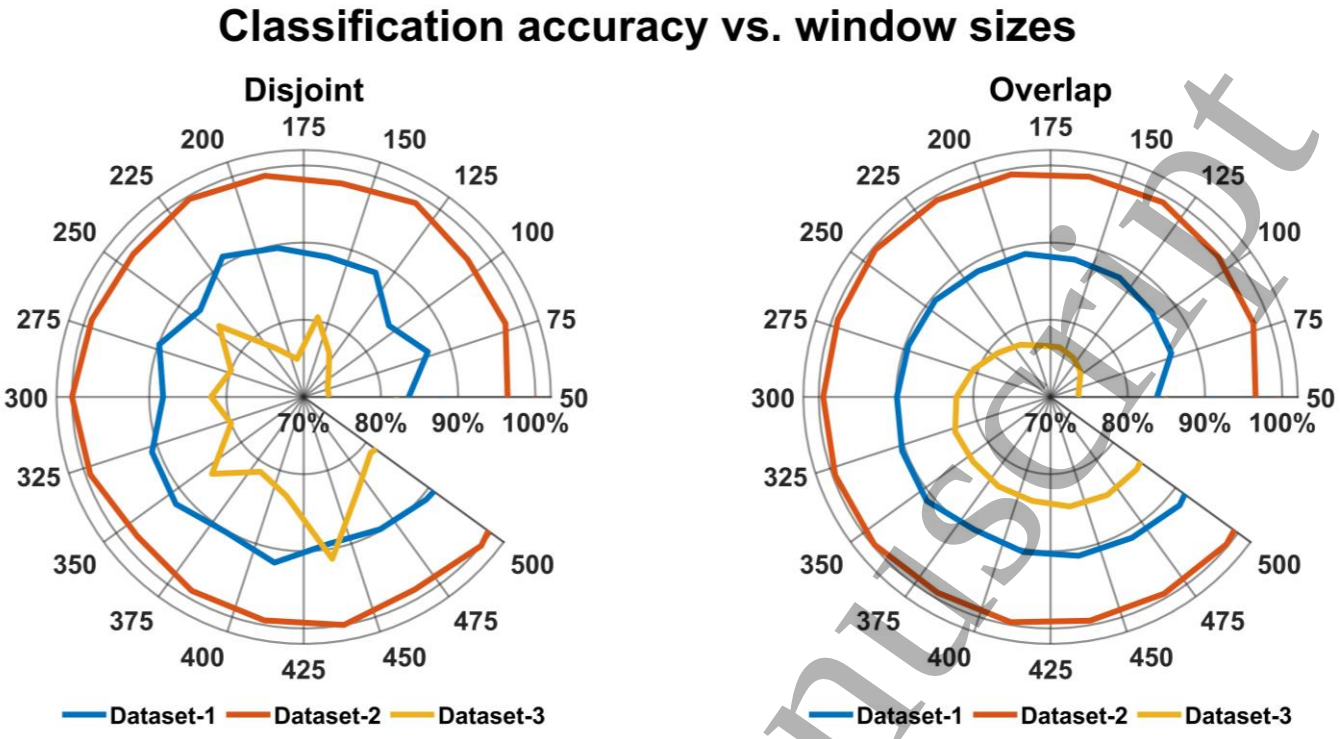

Figure 6. CA vs. window sizes for disjoint and overlap windowing. Relationship between CA and length of disjoint segments for all datasets (Left). Relationship between CA and length of window size for overlap windowing (Right).

For overlap windowing technique, the MSR gradually increased with an increment in window size for all datasets. The highest MSR of 91.87%, 94.20% and 91.39% resulted from window size of 250ms, 150ms and 150ms for dataset-1, dataset-2 and dataset-3, respectively. However for all datasets a slight decrease in MSR has been observed after increasing window size from 275ms, 250ms and 225ms for dataset-1, dataset-2 and dataset-3, respectively. The MSR of window size of 250ms for dataset-1 is significantly different from MSR of all investigated window sizes except 125ms, 225ms and 250ms (P-values > 0.05). Similarly, the MSR of 150ms for dataset-2 is significantly different from MSR of all investigated window sizes except 50ms, 100ms, 125ms, 200ms and 225ms (P-values > 0.05). For dataset-3, the MSR of 150ms is statistically different from MSR of all investigated window sizes except 75ms and 100ms (P-values > 0.05). In regards with CA, for dataset-1, the lowest and highest MMCAs were observed at window size of 50ms and 450ms with MMCA of 83.77%±0.55 and 91.82%±1.04, respectively. Varying the length of window size from 50ms to 275ms changes MMCA significantly, beyond 275ms there is no significant change in MMCA. Two-way ANOVA revealed that MMCA of window size 450ms, highest observed MMCA in dataset-1, is significantly different from MMCAs of window sizes of 50ms to 275ms (P-values < 0.05). For dataset 2, the minimum and maximum MMCAs were observed at window size of 50ms and 225ms with MMCAs of 96.55±0.32 and 99.64±0.33, respectively. The MMCA for dataset-2 significantly increased with an increment in window size from 50ms to 225ms, and afterwards no further increase in accuracy is observed. For dataset-3, the lowest and highest MCA were observed at window size of 50ms and 400ms with MCA of 73.36% and 91.34%, respectively. The MCA significantly increased from 73.57%±12.2 to 83.06%±9.1 by changing window size from 50ms to 325ms, however, no significant increment in MCA has been observed by increasing window size afterwards.

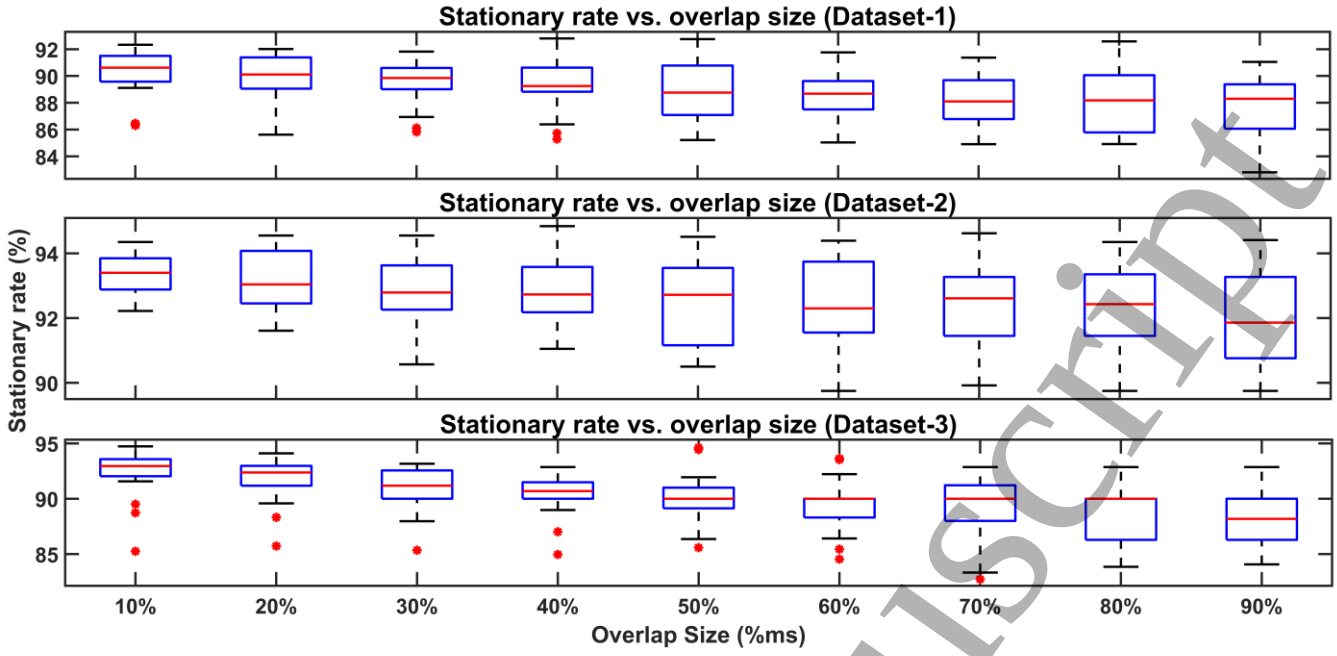

Figure 7. MSR vs. Overlap size for overlap windowing technique against all datasets. The graph shows relationship between MSR and length of overlap size for all datasets. An increase in length of overlap size results in a decrease in MSR for all datasets.

3.2 Optimum overlap size for overlap windowing

The results of MSR and MCA with respect to overlap size, for overlap windowing, are summarized in figure 7 and 8, respectively. Both MSR and MCA depicted an inversely proportional relationship with overlap size. The maximum MSR of 90.16%, 93.36% and 92.28% were yielded from overlap size of 10% for dataset-1, dataset-2, and dataset-3, respectively. The MSR of overlap size of 10% was significantly different from MSR of overlap sizes of 50% and onwards, 60% and onwards and 40% and onwards, for dataset-1, dataset-2, and dataset-3, respectively (P-values < 0.05). No significant difference in MSR of overlap sizes is observed except those which are mentioned explicitly for all datasets (P-values > 0.05).

The maximum MCA of 90.2%, 99.3% and 78.92% were yielded from overlap size of 10% for dataset-1, dataset-2, and dataset-3, respectively. The MCA of overlap size of 10% was significantly different from MCA of overlap sizes of 50% and onwards, for dataset-1. However, no significant differnce in MCA of all overlap sizes existed for dataset-2 and dataset-3 (P-values > 0.05).

Combinedly, on all datasets, MSR of overlap size of 10% outperformed all investigated overlap sizes (P-values < 0.05) but no significant difference with MSR of overlap size of 20% existed (P-value > 0.05). Similarly, on all datasets combinedly, the MCA of overlap size of 10% was significantly higher and different from MCA of all overlap sizes (P-value < 0.05) except 20% and 30% (P-values > 0.05).

3.3 Disjoint vs. overlap windowing

With respect to MSR, on all investigated window and overlap sizes, it was observed that overlap windowing has higher MSR compared to disjoint technique. Figure 9 depicts the comparative bar graphs for both windowing techniques, it can be observed that, on each individual window size overlap windowing has better CA results compared to the disjoint windowing technique. Statistically, overlap windowing (on all overlap sizes) outperforms disjoint windwoing technique in terms of MSR for both dataset-1 and dataset-3 (P-values < 0.05). However, for dataset-2, the MSR of overlap windowing is significantly superior than disjoint windowing at overlap sizes of 10% to 40% (P-values < 0.05) and no significant difference was observed at overlap sizes of 50% and onwards (P-values > 0.05).

Regarding MCA, in dataset-1, overlap window outperformed disjoint window corresponding to overlap sizes of 10% (P-value = 0.0125) and 20% (P-value = 0.0201). However, no statistically significant difference in MCAs of disjoint and overlap windwoing corresponding to overlap size of 30% to 90% was observed (P-values > 0.05). In dataset-2, the MCA of overlap windows outperformed their corresponding disjoint windows with overlap sizes of 10% to 50% (P-values < 0.05). However, no significant difference in

MCA of both schemes exists with overlap size of 60% to 90% (P-values > 0.05). For dataset-3, the MCA of overlap windows outperformed their corresponding disjoint windows with overlap sizes of 10% to 40% (P-values < 0.05) and no significant difference in MCA of both schemes observed with overlap size of 50% to 90% (P-values > 0.05).

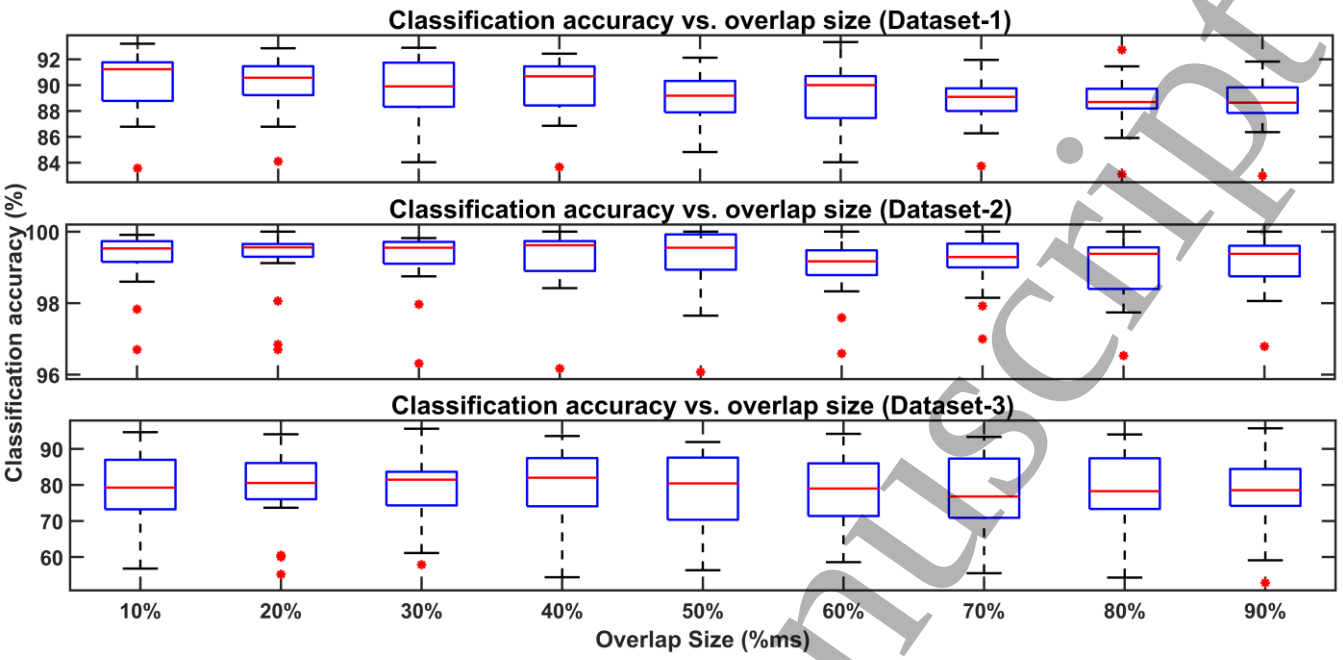

Figure 8. CA vs. Overlap size for overlap windowing technique against all datasets. The graph shows relationship between CA and length of overlap size for all datasets. An increase in length of overlap size results in a decrease in CA for all datasets.

The results of the both techniques were also analyzed statistically by combining all datasets to draw the conclusive remarks about performance of the both techniques in regards with both MSR and MCA. The two-way ANOVA showed that the overlap windowing technique outperformed disjoint windowing on investigated overlap sizes (P-value < 0.05). Whereas, in regards with MCA the performance of overlap windowing corresponding to overlap size of 10% (P-value = 0.0019), 20% (P-value = 0.0047), 30% (P-value = 0.0350) and 40% (P-value = 0.0133) is significantly different from MCA of disjoint windowing technique. Whereas, for all datasets, there is no statistically significant difference in performance of disjoint and overlap windowing technique with overlap size of 50% to 90% (P-values > 0.05).

4. Discussion

The The aim of the conducted study was to identify and investigate best possible windowing configuration for an iEMG-based analysis, diagnosis, and detection system with respect to stationarity rate and classification accuracy. For the said purpose, the data was preprocessed to eliminate unwanted noise from the recorded signals. From figure 2, it is evident that, the applied digital filters denoised the signals significantly. Both windowing techniques, disjoint and overlap, along with varying window sizes were investigated on three independently recorded datasets of iEMG signals. The effect of varying overlap size in overlap windowing technique on stationarity and performance of the system has also been studied and investigated. For offline analysis of EMG signals and to design a system that can classify EMG signals, length of window size should also be in accordance with restriction of delay time in real-time operation. The system designed for offline analysis can be deployed in a device for real-time operations.

For disjoint windowing technique, on all datasets combindely, the MSR increased significantly from 87.08% to 89.96% by changing window size from 50ms to 250ms and decreased significantly afterwards. The MCA increased significantly with by increasing window size for all datasets. Two-way ANOVA revealed that, the MCA increased significantly from 89.27% to 94.83% when length of window size is varied from 50ms to 200ms (P-values < 0.05). No significant difference in MCA was observed afterwards (P-values > 0.05). For overlap windowing technique, on all datasets combindely, the MSR increased significantly from 87.93% to 92.41% by changing window size from 50ms to 225ms and decreased significantly afterwards. Statistical analysis showed that MMCA significantly increased from 90.16% to 94.56% when length of window size is varied from 50ms to 225ms for all iEMG datasets. In MMCA of

window size of 225ms and onwards, no statistically significant difference was observed (P-values > 0.05).

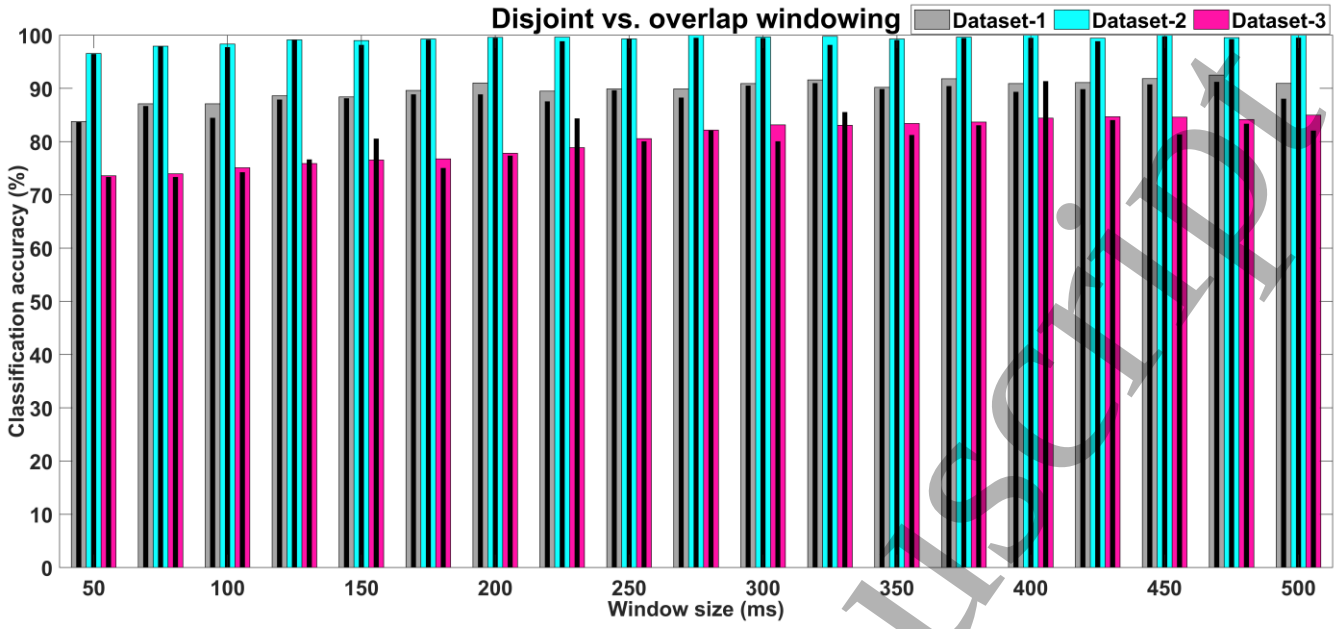

Figure 9. Comparison of MCA for overlap and disjoint windowing techniques for all datasets on all 19 different window sizes. It can be observed that on each individual window size, the overlap windowing technique outperforms disjoint windowing technique in terms of MCA.

The results suggest that optimum window sizes range from 200ms to 300ms and 225ms to 300ms for disjoint and overlap window techniques, respectively, with respect to both stationarity rate and performance of the designed system while acknowledging real-time restriction of length of segment size. The deduced results are in accordance with principles of operation of real-time control systems. As described in [41], for a real-time control system, used in a rehabilitative and assistive robotic devices, window size should be less 300ms. Nevertheless, the proposed optimum window sizes for both disjoint and overlap techniques are slightly lower (3-6%) from sEMG based control systems. Further studies can be conducted to investigate how this small difference in window size impacts the real-time performance of EMG based applications.

The effect of overlap size on MSR and MCA has also been investigated for overlap windowing technique. It is observed that both MSR and MCA are inversely correlated with length of the overlap size. The results revealed that for all datasets (individually and combined), MSR and MCA decreas when overlap size is increased from 10% to 90%. For all datasets (individually and combined) maximum MSR and MCA resulted at overlap size of 10% of any investigated window size. Combinedly, on all datasets, MSR of overlap size of 10% outperformed all investigated overlap sizes (P-values < 0.05), but, no significant difference with MSR of overlap size of 20% existed (P-value > 0.05). Similarly, on all datasets combinedly, the MCA of overlap size of 10% was significantly higher and different from MCA of all overlap sizes (P-value < 0.05) except 20% and 30% (P-value > 0.05).

In comparison between overlap and disjoint windowing schemes with respect to MSR and MCA, it was observed that overlap window has better results. The results of the both techniques were also analyzed statistically by combining all datasets to draw the conclusive remarks about performance of the both techniques in regards with both MSR and MCA. The two-way ANOVA showed that the overlap windowing technique outperformed disjoint windowing on investigated overlap sizes (P-value < 0.05). Whereas, in regards with MCA the performance of overlap windowing corresponding to overlap size of 10% (P-value = 0.0019), 20% (P-value = 0.0047), 30% (P-value = 0.0350) and 40% (P-value = 0.0133) is significantly different from MCA of disjoint windowing technique. Whereas, for all datasets, there is no statistically significant difference in performance of disjoint and overlap windowing technique with overlap size of 50% to 90% (P-value > 0.05). The deduced results are in accordance with results of aforementioned studies, suggesting that for an iEMG based detection and diagnosis system the overlap windowing technique yields better results. For simiplicity and less computational requirements only LDA was used, however, more classifiers can be used to investigate optimum windowing configurations. As the study was conducted offline, in future, the presented results should be tested on a real-time iEMG based control system for

validation. Also, inclusion of more subjects in investigation can also yield more robust results.

5. Conclusion

The study investigated and presented best possible windowing configurations for an iEMG-based diagnosis, detection, and control system based on stationarity rate and performance of the system. Three independently recorded datasets (healthy and abnormal) of iEMG signals were used to investigate effects of windowing type, window size and overlap size on the stationarity rate and performance of an iEMG-based analysis system. It has been observed that the MSR and MCA increase with an increment in window size but an increment in length of overlap size decreases both MSR and MCA. Presented results also showed that, the overlap windowing has very consistent and superior results as compared to disjoint windowing technique when length of window size is varied. The deduced results can be used to select optimum windowing configurations for any iEMG-based diagnostic, detection, and control system.

Acknowledgements

We are thankful to Higher Education Commission (HEC) of Pakistan for funding this project under grant# 10238/Federal/NPRU/RD/HEC/2017.

References

[1] Merletti, R. and Farina, D., 2009. Analysis of intramuscular electromyogram signals. Philosophical Transactions of the Royal Society A: Mathematical, Physical and Engineering Sciences, 367(1887), pp.357-368.

[2] Geselowitz, D.B., 1967. On bioelectric potentials in an inhomogeneous volume conductor. Biophysical journal, 7(1), pp.1-11.

[3] Merletti, R. and Parker, P.J. eds., 2004. Electromyography: physiology, engineering, and non-invasive applications (Vol. 11). John Wiley & Sons.

[4] Nair, S.S., French, R.M., Laroche, D. and Thomas, E., 2009. The application of machine learning algorithms to the analysis of electromyographic patterns from arthritic patients. IEEE Transactions on Neural Systems and Rehabilitation Engineering, 18(2), pp.174-184.

[5] Waris, A., Zia ur Rehman, M., Niazi, I.K., Jochumsen, M., Englehart, K., Jensen, W., Haavik, H. and Kamavuako, E.N., 2020. A Multiday Evaluation of Real-Time Intramuscular EMG Usability with ANN. Sensors, 20(12), p.3385.

[6] Waris, A., Niazi, I.K., Jamil, M., Englehart, K., Jensen, W. and Kamavuako, E.N., 2018. Multiday evaluation of techniques for EMG-based classification of hand motions. IEEE journal of biomedical and health informatics, 23(4), pp.1526-1534.

[7] Goker, I., Osman, O., Ozekes, S., Baslo, M.B., Ertas, M. and Ulgen, Y., 2012. Classification of juvenile myoclonic epilepsy data acquired through scanning electromyography with machine learning algorithms. Journal of medical systems, 36(5), pp.2705-2711.

[8] Koçer, S., 2010. Classification of EMG signals using neuro-fuzzy system and diagnosis of neuromuscular diseases. Journal of Medical Systems, 34(3), pp.321-329.

[9] Waris, A., Niazi, I.K., Jamil, M., Gilani, O., Englehart, K., Jensen, W., Shafique, M. and Kamavuako, E.N., 2018. The effect of time on EMG classification of hand motions in able-bodied and transradial amputees. Journal of Electromyography and Kinesiology, 40, pp.72-80.

[10] Svensson, P., Wijk, U., Björkman, A. and Antfolk, C., 2017. A review of invasive and non-invasive sensory feedback in upper limb prostheses. Expert review of medical devices, 14(6), pp.439-447.

[11] Agnew, W.F. and McCreery, D.B., 1990. Considerations for safety with chronically implanted nerve electrodes. Epilepsia, 31, pp.S27-S32.

[12] Bishop, C.M., 2006. Pattern recognition and machine learning. springer.

[13] Lowery, M.M., Weir, R.F. and Kuiken, T.A., 2006. Simulation of intramuscular EMG signals detected using implantable myoelectric sensors (IMES). IEEE transactions on biomedical engineering, 53(10), pp.1926-1933.

[14] Jochumsen, M., Waris, A. and Kamavuako, E.N., 2018. The effect of arm position on classification of hand gestures with intramuscular EMG. Biomedical Signal Processing and Control, 43, pp.1-8.

[15] Waris, A. and Kamavuako, E.N., 2018. Effect of threshold values on the combination of emg time domain features: Surface versus intramuscular emg. Biomedical Signal Processing and Control, 45, pp.267-273.

[16] Phinyomark, A., Phukpattaranont, P. and Limsakul, C., 2012. Feature reduction and selection for EMG signal classification. Expert systems with applications, 39(8), pp.7420-7431.

[17] Adewuyi, A.A., Hargrove, L.J. and Kuiken, T.A., 2016. Evaluating EMG feature and classifier selection for application to partial-hand prosthesis control. Frontiers in neurorobotics, 10, p.15.

[18] Herberts, P., Kadefors, R., Kaiser, E. and Petersén, I., 1968. Implantation of micro-circuits for myo-electric control of prostheses. The Journal of bone and joint surgery. British volume, 50(4), pp.780-791.

[19] Waris, A., Ur-Rehman, Z.M., Niazi, I.K., Jochumsen, M. and Kamavuako, E.N., 2019. Multi-Day Real-time Myoelectric Control using Intramuscular EMG. In Trent International Prosthetics Symposium (TIPS), 2019.

[20] STEIN, R.B., 1980. New Approaches for the. Bulletin of prosthetics research, 17(33-34), p.51.

[21] Santa-Cruz, M.C., Riso, R.R. and Lange, B., 1999. Natural control of key grip and precision grip movements for a myoelectric prosthesis. Mec, 25-27 August 1999, Fredericton, Canada.

[22] Hargrove, L., Losier, Y., Lock, B., Englehart, K. and Hudgins, B., 2007, August. A real-time pattern recognition based myoelectric control usability study implemented in a virtual environment. In 2007 29th Annual International Conference of the IEEE Engineering in Medicine and Biology Society (pp. 4842-4845). IEEE.

[23] Waris, A., Mendez, I., Englehart, K., Jensen, W. and Kamavuako, E.N., 2019. On the robustness of real-time myoelectric control investigations: A multiday Fitts' law approach. Journal of Neural Engineering, 16(2), p.026003.

[24] Santa-Cruz, M.C., Riso, R.R. and Lange, B., 1999. Natural control of key grip and precision grip movements for a myoelectric prosthesis. Mec, 25-27 August 1999, Fredericton, Canada.

[25] Waris, M.A., Jamil, M., Ayaz, Y. and Gilani, S.O., 2014. Classification of functional motions of hand for upper limb prosthesis with surface electromyography. International Journal of Biology and Biomedical Engineering, 8, pp.15-20.

[26] Goen, A., 2014. Classification of EMG signals for assessment of neuromuscular disorders. International Journal of Electronics and Electrical Engineering, 2(3), pp.242-248.

[27] Subasi, A., Yaman, E., Somaily, Y., Alynabawi, H.A., Alobaidi, F. and Altheibani, S., 2018. Automated EMG signal classification for diagnosis of neuromuscular disorders using DWT and bagging. Procedia Computer Science, 140, pp.230-237.

[28] Yaman, E. and Subasi, A., 2019. Comparison of bagging and boosting ensemble machine learning methods for automated EMG signal classification. BioMed Research International, 2019.

[29] Oskoei, M.A. and Hu, H., 2008. Support vector machine-based classification scheme for myoelectric control applied to upper limb. IEEE transactions on biomedical engineering, 55(8), pp.1956-1965.

[30] Farrell, T.R., 2008. A comparison of the effects of electrode implantation and targeting on pattern classification accuracy for prosthesis control. IEEE Transactions on Biomedical Engineering, 55(9), pp.2198-2211.

[31] Hammond, J.K. and White, P.R., 1996. The analysis of non-stationary signals using time-frequency methods. Journal of Sound and vibration, 190(3), pp.419-447.

[32] Shwedyk, E., Balasubramanian, R. and Scott, R.N., 1977. A nonstationary model for the electromyogram. IEEE Transactions on Biomedical Engineering, (5), pp.417-424.

[33] Xiong, F.Q. and Shwedyk, E., 1987. Some aspects of nonstationary myoelectric signal processing. IEEE transactions on biomedical engineering, (2), pp.166-172.

[34] Ju, K., Itakura, N., Iguchi, Y. and Minamitani, H., 1989, November. Functional analysis of nonstationary EMG signals during a quick movement. In Images of the Twenty-First Century. Proceedings of the Annual International Engineering in Medicine and Biology Society, (pp. 749-751). IEEE.

[35] Beck, T.W., Housh, T.J., Weir, J.P., Cramer, J.T., Vardaxis, V., Johnson, G.O., Coburn, J.W., Malek, M.H. and Mielke, M., 2006. An examination of the runs test, reverse arrangements test, and modified reverse arrangements test for assessing surface EMG signal stationarity. Journal of neuroscience methods, 156(1-2), pp.242-248.

[36] Messaoudi, N., Bekka, R.E.H., Ravier, P. and Harba, R., 2017. Assessment of the non-Gaussianity and non-linearity levels of simulated sEMG signals on stationary segments. Journal of Electromyography and Kinesiology, 32, pp.70-82.

[37] Hudgins, B., Parker, P. and Scott, R.N., 1993. A new strategy for multifunction myoelectric control. IEEE Transactions on Biomedical Engineering, 40(1), pp.82-94.

[38] Thongpanja, S., Phinyomark, A., Quaine, F., Laurillau, Y., Wongkittisuksa, B., Limsakul, C. and Phukpattaranont, P., 2013, August. Effects of window size and contraction types on the stationarity of biceps brachii muscle EMG signals. In 7th International Convention on Rehabilitation Engineering and Assistive Technology (p. 44).

[39] Mebarkia, K., Bekka, R.E.H., Reffad, A. and Disselhorst-Klug, C., 2014. Fuzzy MUAP recognition in HSR-EMG detection basing on morphological features. Journal of Electromyography and Kinesiology, 24(4), pp.473-48

[40] Ashraf, H., Waris, A., Jamil, M., Gilani, S.O., Niazi, I.K., Kamavuako, E.N. and Gilani, S.H.N., 2020. Determination of Optimum Segmentation Schemes for Pattern Recognition-Based Myoelectric Control: A Multi-Dataset Investigation. IEEE Access, 8, pp.90862-90877.

[41] Englehart, K. and Hudgins, B., 2003. A robust, real-time control scheme for multifunction myoelectric control. IEEE transactions on biomedical engineering, 50(7), pp.848-854.

[42] Ortiz-Catalan, M., Brånemark, R. and Håkansson, B., 2013. BioPatRec: A modular research platform for the control of artificial limbs based on pattern recognition algorithms. Source code for biology and medicine, 8(1), p.11.